



**HAL**  
open science

# Including a distribution of threshold displacement damage energy on the calculation of the damage function and electron's Non Ionizing Energy Loss

Christophe Inguibert

► **To cite this version:**

Christophe Inguibert. Including a distribution of threshold displacement damage energy on the calculation of the damage function and electron's Non Ionizing Energy Loss. *Journal of Nuclear Materials*, 2022, 559, pp.153398. 10.1016/j.jnucmat.2021.153398 . hal-03479357

**HAL Id: hal-03479357**

**<https://hal.science/hal-03479357>**

Submitted on 14 Dec 2021

**HAL** is a multi-disciplinary open access archive for the deposit and dissemination of scientific research documents, whether they are published or not. The documents may come from teaching and research institutions in France or abroad, or from public or private research centers.

L'archive ouverte pluridisciplinaire **HAL**, est destinée au dépôt et à la diffusion de documents scientifiques de niveau recherche, publiés ou non, émanant des établissements d'enseignement et de recherche français ou étrangers, des laboratoires publics ou privés.

# Including a distribution of threshold displacement damage energy on the calculation of the damage function and electron's Non Ionizing Energy Loss

C. Inguibert

*ONERA, Toulouse center 2 av. E.Belin 31055 Toulouse cedex, France*

## Abstract

The Norgett-Robinson-Torrens displacements per atom function is commonly used to estimate the amount of atomic displacement produced by incident energetic particles. At low incident energy, this function is defined as a step function presenting a single threshold displacement damage energy. But materials have different threshold as a function of the crystallographic orientation. Molecular dynamic simulations show that a continuously varying damage energy probability is best suited to represent the threshold damage region. This work proposes a method to introduce in the NRT damage function a continuous damage energy distribution. The impact of a change on the damage function in the threshold region is evaluated on the incident electrons' Non Ionizing energy Loss.

*Key words*—Radiative environment, displacement damage, electrons, Non Ionizing Energy Loss, damage function.

---

## 1. Introduction

Materials subject to radiations can undergo significant degradations related to atomic displacements [1-3]. The radiation belts where most of space vehicles revolve or the constraining environment induced in nuclear power plants [4] are a concern. Atomic displacements which is the point here, can result from the slowing down induced by the matter of the charged particles such as protons or electrons present in the space environment [3]. Analogously, fission neutrons, are also an important source of damage for materials located at the core of nuclear fission reactors [4]. In space the reliability of onboard electronics subject to radiations is a real issue. The electronic properties of semiconductor materials are particularly sensitive to the defects production rate, consequence of displacement damage cascade initiated by knock on atoms [1-4]. Hence, the functioning characteristics of electronic components boarded on satellites can significantly drift along the time. These devices can reach their operating limit, which is a real concern for space projects. In nuclear fission reactors the particularly harsh environment raises the question of the mechanical resistance of materials. The estimation of the lifetime of a nuclear reactor pressure vessel subject to very high thermal flux is a particular concern [4].

A process of great importance in the study of radiation damage is the understanding of displacement cascades. When an atom of the material is put into motion and extracted from its lattice site by an incident particle, it will move through the material and create a number of other atomic displacements. These atomic displacements degrade the structure of the irradiated materials and consequently their performances. It is therefore crucial to evaluate the radiative constraint in many applications, and the resulting number of produced atomic displacements that can be a source of degradation. This estimation requires to discriminate along the path of the moving particle, the part of its energy that goes into atomic displacement from the part that induces ionization of the medium. The well-known Lindhard energy partition function  $N_d(E^d)$  provides this physical quantity [5-8]. It is established in the framework of the Binary Collision Approximation (BCA) [1, 2, 4-10]. Most of time it is given for monoatomic materials. Kinchin & Pease [5], and Robinson and Torrens [6, 7] are the most widely used formulations (NRT : Norgett, Robinson & Torrens), that makes possible to know the number of atomic displacements for a given Primary Knock on Atom (PKA) of a given energy  $E$ , assuming a threshold displacement damage energy ( $E^d$ ). For polyatomic materials, Parkin & Coulter [11] established an integro-differential equation governing this number of displacements. This approach takes into account the possibility for atoms of a given specie to dislodge atoms of other species present in the compound [11-14]. These cross terms, that are neglected otherwise, are in that case considered. The number of displacements produced in an irradiated material is incidentally deduced from this partition function by combining it with the nuclear interaction cross sections (coulombian, nuclear elastic and inelastic) [10, 16-21]. It results in a physical quantity known as the displacement cross sections or the Non Ionizing Energy Loss (NIEL) [4, 10, 15-21].

These calculations are based upon the main concept of the threshold displacement damage energy  $E^d$ . The NIEL calculation of a given element often assumes a unique value of  $E^d$ . Polyatomic materials present different threshold displacement damage energies relative to each of their constituting elements [11-14]. This classical approach, despite its simplicity has proven its reliability [3, 4]. But, more recently both Molecular Dynamics (MD) simulations and first principle calculations have been used to study the damaging process more accurately [21-34]. The usage of MD simulations is limited by its complexity. And consequently, such kind of simulations have been fully performed for a quite limited number of materials, still offering to the NRT approach fine days ahead. However, the accuracy of the binary cascade approximation is discussed [4]. A new displacement production estimator (athermal recombination corrected dpa, arc-dpa) extending the NRT approach has been

proposed [4, 8]. It provides a more physically realistic descriptions of primary defect creation in materials. But the threshold displacement energy region remains complex to model and a large uncertainty exist in the choice of the  $E^d$  value. It is widely reported in the literature [4, 21-36] and references in there, that the NRT approach presents different shortcomings and specifically near the threshold region for low PKA energies. MD simulations clearly demonstrate that the probability to displace an atom increases gradually rather than having an abrupt threshold [4]. A damage function transitioning directly from zero to one at a given  $E^d$  is not relevant to describe the damaging mechanism in the threshold region [4]. The definition of  $E^d$  within the framework of the NRT approach is thus crucial. Often an average value is chosen.  $E^d$  can be averaged over all the crystallographic directions. However, the use of a single threshold displacement energy to describe the damaging cascade process is admitted to be a rough approximation [4, 21-36]. Some recent MD papers have proven the existence of a continuous distribution of  $E^d$  values, even in monoatomic materials [4, 36-39]. Indeed, the threshold displacement energy depends on the direction of the moving PKA in the medium. To remain in the scope of the BCA, average or “effective” threshold displacement energies have been evaluated and used for many materials [36]. Correction factors have been proposed to improve the reliability of the energy partition function [4, 8, 36]. Some other attempts to estimate this function using MD simulations have also been proposed [40, 41]. Ref. [41] proposes to introduce in the arc-dpa model, a minimum displacement damage energy  $E_{\min}^d$  to change the classical step function at  $E^d$ , to a smooth increasing function between  $E^d$  and  $E_{\min}^d$ . But the impact of a distribution of  $E^d$  values rather than a single one has not been studied in detail. The work presented here proposes, remaining in the NRT approach, to introduce a continuous probability of damage energy. It aims at better describe the threshold displacement region of the NRT damage function. This method allows to include in the NIEL calculation the dependence of the threshold displacement energy with the crystallographic directions. The impact of a full displacement damage energy distribution, going from a minimum up to a maximum  $E^d$  values on both the NIEL and the damage function is analysed. A focus will be made on the electron NIELs which is demonstrated to be quite sensitive to the threshold region [19]. Calculations will be performed on carbon and copper materials for which the damage function is known close to the threshold. It has been estimated with MD simulations for carbon [37] and measured experimentally for copper [4]. The analysis is also performed for silicon material for which experimental damage factor can be compared to the calculated NIEL [42]. First, we will introduce the method employed to take into account a distribution of  $E^d$  in both the damage function and the NIEL calculation. Second, the results will be discussed in the cases of carbon, copper and silicon target materials.

## 2. Classical displacement damage cascade modelling

When an energetic particle such as an electron, a proton an heavy ion or a neutron enters a solid, it transfers a part of its energy to the nuclei of the atoms of the solid. The rest of its energy is given to the electrons of the medium during ionizing processes. At high energy (MeV), electronic losses dominate while at lower energy ( $\sim$  keV) this is elastic nuclear losses. An elastic collision can put into motion an atom of the solid, which in turn can displace neighboring atoms, thus creating a cascade of displacements. Since not all displaced atoms can return to their original site, or to an equivalent site, this cascade results in the creation of vacancies and interstitials: also called Frenkel pairs. The accumulation of these defects can eventually lead to a change in the properties of the material. To describe this cascade, one must study the behavior of the first impacted atom (PKA). This PKA will in turn displace other atoms of the target if its kinetic energy is sufficient (greater than  $2E^d$ ). The quantification of the number of displacements can thus be restricted to the study of the cascades initiated by the PKA (NRT function). The NRT function is classically given by :

$$N_d(E) = \begin{cases} 0 & \text{if } E_{\text{Damage}} < E^d \\ 1 & \text{if } E^d \leq E_{\text{Damage}} < \frac{2 \cdot E^d}{0.8} \\ \frac{0.8 \cdot E_{\text{Damage}}}{2 \cdot E^d} & \text{if } \frac{2 \cdot E^d}{0.8} \leq E_{\text{Damage}} \end{cases} \quad (1)$$

Where  $E_{\text{Damage}}$  is provided by Robinson's expression [6, 7]. This approach assumes a single threshold displacement damage energy while it is known that the displacement damage energy threshold varies along the crystallographic directions, resulting in a distribution of damage energy for a material [37-39]. The NRT function is the solution of an integro-differential equation [11] laying on the assumption that along the cascade of shocks, recoil nuclei will encounter atoms of identical nature having a single damage energy  $E^d$ . But it is possible to solve this integro-differential equation assuming different  $E^d$  values. This problem has already been solved by Parkin & Coulter [11] for compound target material. Those authors solve the damage cascade equation by taking into account atoms of different nature having different threshold displacement damage energy. A slightly simpler analogous approach can be followed, just assuming atoms of identical nature but having different damage energies. It is assumed that the collisions that have taken place along a given crystallographic direction are equivalent to a collision with an atom having a certain damage energy. It requires to get the dependence law between the threshold displacement energy and the crystallographic direction, or to make some assumptions if this information is not available for the studied material. This way, and according to some hypothesis on the damage energy distribution, the NRT partition function can be estimated including various threshold displacement damage energies. The integro-differential equation of Parkin & Coulter underlying this method is described in the following section.

### 3. Parkin & Coulter integro differential equation

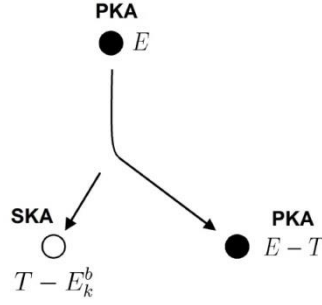


**Fig. 1.** Schematic of the interaction of a PKA with a SKA

In this section we are going to remind the principle of the Parkin and Coulter approach to calculate the energy partition function of a compound target material. Its adaptation to the case where a distribution of  $E^d$  values is employed is described in a second time. Let be a material composed of atoms of type  $i$  and type  $j$ . One can introduce [11] two functions called total displacement function and net displacement function, denoted respectively  $n_{ij}$  and  $\bar{g}_{ij}$ . These two functions characterize the number of displacements produced in a cascade. The quantity  $n_{ij}(E)$  is defined as the average number of type  $j$  atoms which are at any time displaced from their site in a displacement cascade initiated by a type  $i$  PKA of energy  $E$ . The function has a minimum value of 1 because the initial PKA is counted by default. The quantity  $\bar{g}_{ij}(E)$  is defined as the average number of type  $j$  atoms which are at any time displaced and not recaptured by replacement collisions, in a cascade of displacements initiated by a type  $i$  PKA. Similarly to  $n_{ij}(E)$ ,  $\bar{g}_{ij}(E)$  counts the PKA.

Let us consider a PKA of the type  $i$  initially dislodged from its site by an incident particle (Fig. 1). Along its path  $dx$ , this PKA will eventually create  $n_{ii}$  displacements of atoms of type  $i$ , and  $n_{ij}$  displacements of atoms of type  $j$ . Likewise, a  $j$  type PKA will produce  $n_{jj}$  and  $n_{ji}$  atomic displacements. The conservation of the number of atoms within the material implies that each of these numbers of displacements is conserved. In other words,  $n_{ij}$  is conserved before and after the interaction.  $\bar{n}_{ij}(E) = n_{ij}(E) - \delta_{ij}$ , which is the function corresponding to  $n_{ij}$ , but which excludes the PKA from the counting is written by Parkin and Coulter [11] as follow :

$$\begin{aligned} \bar{n}_{ij}(E) = & \sum_k \int_0^{\Lambda_{ik} \cdot E} \{ \rho_k(T) \cdot (\delta_{kj} + \bar{n}_{kj}(T - E_k^b)) + [1 - \lambda_{ik}(E - T) \cdot \rho_k(T)] \bar{n}_{ij}(E - T) \} N_k \frac{d\sigma_{ik}(E, T)}{dT} dx dT \\ & + \int_0^{T_{em}} \bar{n}_{ij}(E - T_e) \cdot N_e \frac{d\sigma_{ie}(E, T)}{dT} dx dT \\ & + \left( 1 - \sum_k N_k \sigma_{ik}(E) dx - N_e \sigma_{ie}(E) dx \right) \bar{n}_{ij}(E) \end{aligned} \quad (2)$$

The sum over  $k$  relate to the different types of atom composing the target material.  $\Lambda_{ik} = \frac{4A_i \cdot A_k}{(A_i + A_k)^2}$ , with  $A_{i,k}$  which are the atomic mass of the colliding nuclei.  $\rho_k(T)$  is the probability to dislodge an atom of the type  $k$  from its lattice site when the energy transfer during the collision is equal to  $T$ .  $\lambda_{ik}(E - T)$  is the probability that a type  $i$  atom of energy  $E$ , having a residual energy  $E - T$  after knocking and displacing a  $k$  type atom to being trapped at the lattice site of  $k$  atom.  $\delta_{kj}$  is the Kronecker function.  $E_k^b$  is the binding energy lost during the displacement of a  $k$  type atom (Fig. 1).  $T_{em}$  is the kinetic energy transferred to the electrons of the medium.  $T_e$  is the ionizing energy,  $N_k$  the atomic density for  $k$  type atoms and  $N_e$  the electronic density of the medium.  $\frac{d\sigma_{ik}(E, T)}{dT}$  is the differential interaction cross section for an  $i$  type atom of energy  $E$  to transfer the energy  $T$  to a recoil nuclei of type  $k$ , and  $\frac{d\sigma_{ie}(E, T)}{dT}$  is the differential interaction cross section for an  $i$  type atom of energy  $E$  to transfer the energy  $T$  to an electron of the medium.  $\sigma_{ik}(E)$  is the type  $i$  + type  $k$  nuclear interaction cross section and  $\sigma_{ie}(E)$  is the total electronic interaction cross section.

The first integral in equation 2 represents over the distance  $dx$ , the number  $\bar{n}_{ij}$  of  $j$  type atoms displaced by an  $i$  type PKA, taking into account all SKAs (Secondary Knocked on Atom) of  $k$  type.  $\delta_{kj}$  gives the contribution for a  $k$  type atom displaced by a  $j$  type atom. It is considered that the displaced atom  $k$  having energy  $T - E_k^b$  produces displacements of the type  $j$ :  $\bar{n}_{ij}(T - E_k^b) \cdot \bar{n}_{ij}(E - T)$

is the contribution of the type  $i$  nucleus having a recoil energy  $E-T$ , provided that this one is not captured (probability  $[1-\lambda_{ik}(E-T) \cdot \rho_k(T)]$ ).

The second integral represents the case for which the PKA interacts along its path with the electrons of the medium. That means that the energy of the PKA is changed along the path  $dx$  and it has to be taken into account in the evaluation of the number of  $j$  type displaced atoms which is given for a PKA of a given energy. The last term represents the cases for which no interaction has occurred along the path. It represents the conservation of  $n_{ij}$  weighted to the probability that no interaction occurs along the path  $dx$ .

In order to simplify this equation, the second term will be rewritten introducing the stopping power of the PKA. If we assume that along the path  $dx$  the energy transferred to the electrons in the medium is low compared to the energy  $E$  of the PKA,  $\bar{n}_{ij}(E-T_e)$  can be rewritten as follow:

$$\bar{n}_{ij}(E-T_e) = \bar{n}_{ij}(E) - T_e \frac{d\bar{n}_{ij}(E)}{dE} + o(E) \quad (3)$$

By introducing the electronic stopping power of atomic specie  $i$  of the target material  $S_{ie}$ , as well as the atomic fraction of the species  $k$ :

$$s_{ie}(E) = \frac{1}{N} \int_0^{T_{em}} T_e N_e \frac{d\sigma_{ie}(E,T)}{dT} dT \quad (4)$$

with  $f_k = \frac{N_k}{N}$  and  $N$  being the atomic density of the  $k$  atoms, we get for equation (2) after rearranging the different terms:

$$\begin{aligned} s_{ie}(E) \frac{d\bar{n}_{ij}(E)}{dE} &= \sum_k f_k \int_0^{\Lambda_{ik} \cdot E} \{ \rho_k(T) \cdot (\delta_{kj} + \bar{n}_{kj}(T - E_k^b)) \\ &+ [1 - \lambda_{ik}(E-T) \cdot \rho_k(T)] \bar{n}_{ij}(E-T) \\ &- \bar{n}_{ij}(E) \} \frac{d\sigma_{ik}(E,T)}{dT} dT \end{aligned} \quad (5)$$

The same principles apply for the net displacement function, which then results in the following integro-differential equation:

$$\begin{aligned} s_{ie}(E) \frac{dg_{ij}(E)}{dE} &= \sum_k f_k \int_0^{\Lambda_{ik} \cdot E} \{ \rho_k(T) \cdot g_{kj}(T - E_k^b) \\ &+ [1 - \lambda_{ik}(E-T) \cdot \rho_k(T)] g_{ij}(E-T) \\ &- g_{ij}(E) \} \frac{d\sigma_{ik}(E,T)}{dT} dT \end{aligned} \quad (6)$$

The difference between equation (6) governing  $g_{ij}$  and equation (5) governing  $\bar{n}_{ij}$  comes from the kroneker function  $\delta_{kj}$  presents in equation (5) and not in (6).  $n_{ij}$  counts all atoms of type  $j$  that are displaced, including also those that are instantly trapped in a replacement process. The function will be less representative of the final degradation. This is why we will focus on the later function  $g_{ij}$  in the rest of the paper.

#### 4. Numerical resolution

To solve the equation (5) and (6) presented in the previous section, the Runge-Kutta (RK4) method has been used. The ion/ion interaction cross sections are the one of ZBL [43]. The used electronic energy loss are those of SRIM [43, 44]. The displacement damage probability  $\rho_k(T)$  and the probability of capture  $\lambda_{ik}(E-T)$  are defined as follow:

$$\rho_k(T) = \begin{cases} 0 & \text{if } T < E_k^d \\ 1 & \text{if } T \geq E_k^d \end{cases} \quad (7)$$

$$\lambda_{ik}(T) = \begin{cases} 1 & \text{if } T < E_{ik}^{cap} \\ 0 & \text{if } T \geq E_{ik}^{cap} \end{cases} \quad (8)$$

In these formulas  $E_k^d$ , the threshold displacement damage energy, is the average kinetic energy that a k type atom must receive to be removed from its site.  $E_{ik}^{cap}$  is the capture energy. This is the average residual energy, below which a type i atom which has just interacted with a k type atom, becomes trapped at the vacant site left by the k recoil nuclei in the lattice. In our simulations  $E_{ik}^{cap}$  have been taken equal to  $E_k^d$ . Usually, in the NRT approach, a single value of  $E_k^d$  is chosen for each k type atom of the compound material. For a monoatomic material a single value is chosen (21 eV for silicon for instance). Our goal here is to introduce for monoatomic materials different values for  $E_k^d$  to analyse the impact of this parameter first on the damage function and second on the NIEL. Both discrete values and a continuous distribution will be analysed.

Some boundary limits are required to solve the integro-differential equations. They have been chosen as follow. These conditions are quite simple given the definitions taken for  $n_{ij}(E)$  and  $g_{ij}(E)$ . Both  $n_{ij}(E)$  and  $g_{ij}(E)$  are equal to  $\delta_{ij}$  if the energy E of the PKA is lower than the displacement threshold (9). The threshold displacement damage energy being different for each j type recoil, the following formulation has been chosen:

$$\left. \begin{aligned} n_{ij}(E) &= \delta_{ij} \\ g_{ij}(E) &= \delta_{ij} \end{aligned} \right\} \text{if } 0 \leq E \leq E_j^d \quad (9)$$

The calculation has been validated by comparison with the simulation performed for SiC material in ref. [14].

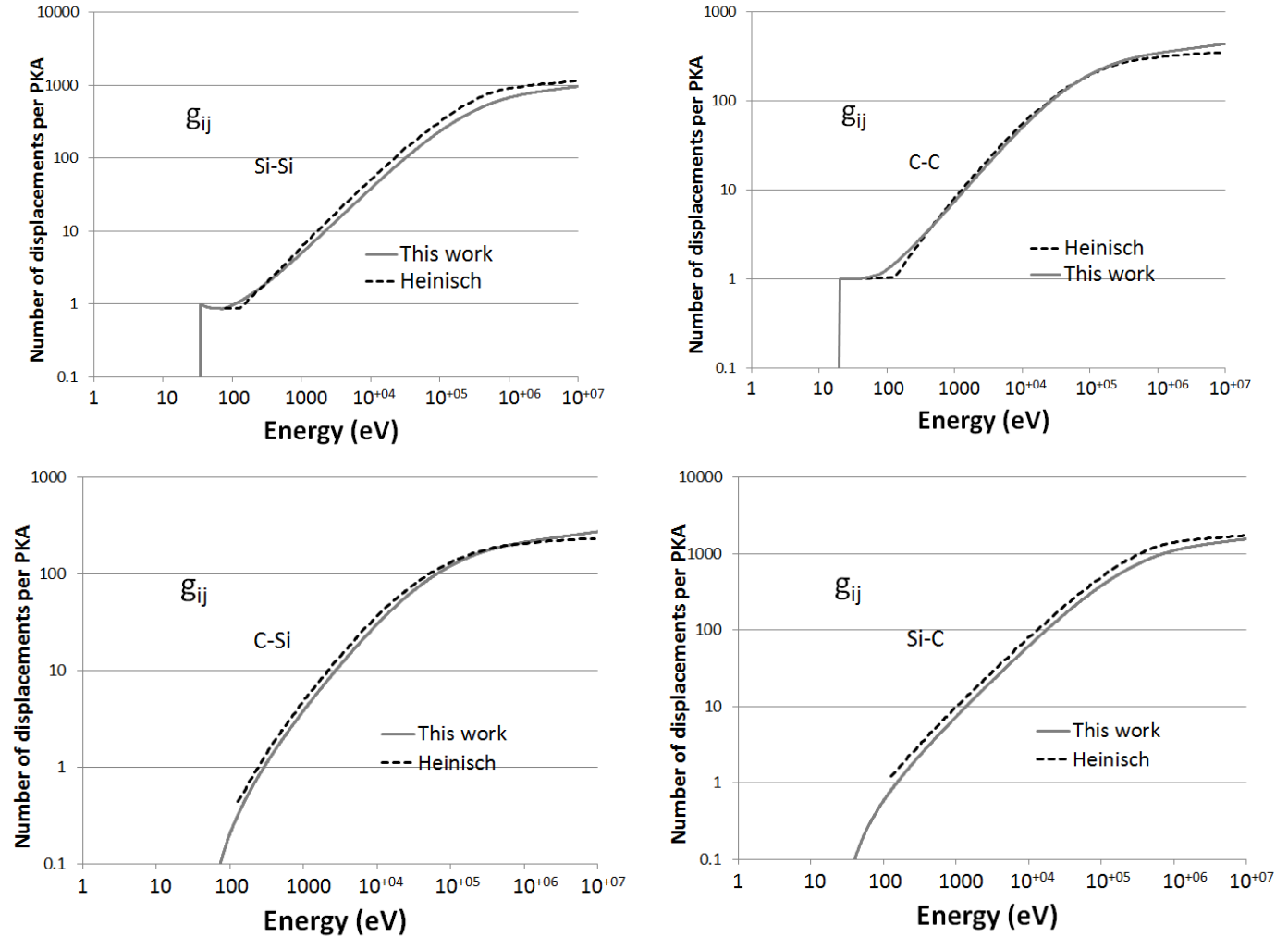


**Fig. 2.** Net number of displacement  $g_{ij}$  calculated for SiC couples following equation (6). Comparison with calculation of [14]. The threshold displacement damage energies are for each couple 41 eV (C/Si), 35 eV (Si/Si), 24 eV (Si/C) and 20 eV (C/C).

The number of displacements found by this method is in agreement with molecular dynamic simulations performed on SiC [45]. One can identify two different behaviors in Fig. 2. Some functions tend gradually to zero while some others present a minimum value of 1. The number of atomic displacements is forced to 1 by the boundary condition at the beginning of the simulation,

when identical types of atoms are considered. Indeed, the PKA is counted as the first displacement. Reversely the number of displaced atoms tends to zero when the displaced atoms are of a « different » nature from the PKA. In that case the PKA must not be counted among the other displaced atoms as it is from a different nature. This number of displaced atoms increases gradually with the energy of the PKA, while The number of displaced atoms remains close to one when recoil atoms of the same nature of the PKA are considered. This number, as can be seen on the Fig.2 (Si-Si case) not remains exactly equal to 1. It decreases slightly when the i type PKA start to displace j type atoms (Fig. 2, Si-C case). The i type PKA loses a significant part of its energy and is re-trapped making the number of i type atoms slightly decrease.

### 5. Average net displacement damage function for a monoatomic target material: cases of carbon and copper

The approach shown previously have been applied to monoatomic materials just assuming different threshold displacement damage energies. It is as if there is different population of atoms having different binding energies. The calculation requires the knowledge of the damage energy distribution  $dP/dE^d$ . The energy required to dislodge an atom from its lattice site depends on the direction of the collision and thus on the variation of the displacement energy as a function of the angle :  $dEd/d\Omega$ . The damage energy distribution probability is thus given by  $dP/dE^d = (dP/d\Omega)/(dEd/d\Omega)$ . After several collisions, the momenta of the recoil atoms become randomized, we will assume in a first approximation that all recoil nuclei are ejected isotopically ( $dP/d\Omega=\text{constant}$ ). The calculation is thus as if each SKA is put into motion in a different crystallographic direction.

Let us consider the case of a volume of a given monoatomic material (carbon for instance). Similarly to a compound material let's assume that there is three different type of carbon atoms (C1, C2, C3), having respectively three different damage energies ( $E_1^d, E_2^d, E_3^d$ ). The algorithm shown previously provide the number  $n_{i,j}$  of j type atoms displaced by i type PKA. This PKA, will produce  $n_i$  atomic displacements whatever the nature and binding energy of the SKAs :

$$n_i = \sum_{j=1}^3 n_{i,j} \quad (10)$$

Where j varies from 1 to 3 if we consider 3 different carbon atoms having three different damage energies. The average number of atomic displacements produced by a PKA, whatever its type and its damage energy is thus simply given by :

$$n = \sum_{i=1}^3 dP_i \cdot n_i \quad (11)$$

Where  $dP_i$  is simply the probability to encounter an atom of type i (with damage energy  $E_i^d$ ). This probability is linked with the probability to eject a PKA in a way that its binding energy is  $E_i^d$ . In this example we consider only three different damage energy, but, the recoil nuclei are ejected along a continuous angular distribution representative of the coulombian interaction. By going through the continuous limit, assuming a distribution of displacement energy  $dP/dE^d$  going from  $E_{\min}^d$  to  $E_{\max}^d$ . The net displacement damage function can be rewritten :

$$n(E) = \int_{E_{\min}^d}^{E_{\max}^d} \frac{dP}{dE^d} \cdot n_{E^d}(E) \cdot dE^d \quad (12)$$

In that case SKAs are assumed to be ejected isotopically. This hypothesis is supported by the fact that, in such kind of random process, the angular directions of moving particles randomize and distribute from generation to generation more and more homogeneously among all the directions. It tends toward an isotropic distribution. This approximation is particularly relevant for polycrystalline materials where there is no preferential crystallographic orientation. This is also the underlying assumption of the NRT damage function where all crystal orientations are taken into account thanks to the use of a mean unique damage energy.

A calculation has been performed in the case of graphite. First, only three types of carbon atoms having three different displacement energies (25 eV, 37.5 eV and 50 eV) have been chosen for the calculation. That leads to 9 couples of interactions (Fig. 3). In this case, only carbon PKAs are considered. Even if the energies needed to displace them were different because they have been ejected along different directions they are perfectly equivalent. The capability of these PKAs to displace atoms is obviously independent of the energy required to displace them. They thus displace the same amount of carbon atoms of a given threshold displacement energy. As a consequence, C50-C37.5, C25-C37.5 curves of Fig. 3 are superimposed. Similarly C50-C25 and C37.5-C25 as well as C25-C50 and C37.5-C50 curves overlap. The total number of displacements is simply the sum of the net displacement functions of each recoil atom types (equation 10). This three functions are represented in the right panel of the Fig. 3 by the net displacement function with their respective steps at 25 eV, 37.5 eV and 50 eV. The full net displacement function that includes all the atoms of different types (equation 11) is also represented. A constant  $dP/dE^d$  distribution in the range [25 eV, 50 eV] [37] has been chosen for the calculation. Most of  $E^d$  values reported in the literature for carbon material are in this energy domain [37, 46]. In that case, and according to our hypothesis, the probabilities to strike a carbon atom of each different types (different damage energy) are equal. That leads to a net displacement function presenting three increasing steps at 25 eV, 37.5 eV and 50 eV. The NRT single step function is replaced near the threshold by a three steps function. Going through the continuous limit leads to smooth the damage function near the threshold (dotted line in right panel of Figure 3). In that calculation, the continuous distribution of probability  $dP/dE^d$  has been chosen constant in the range [25 eV, 50 eV]

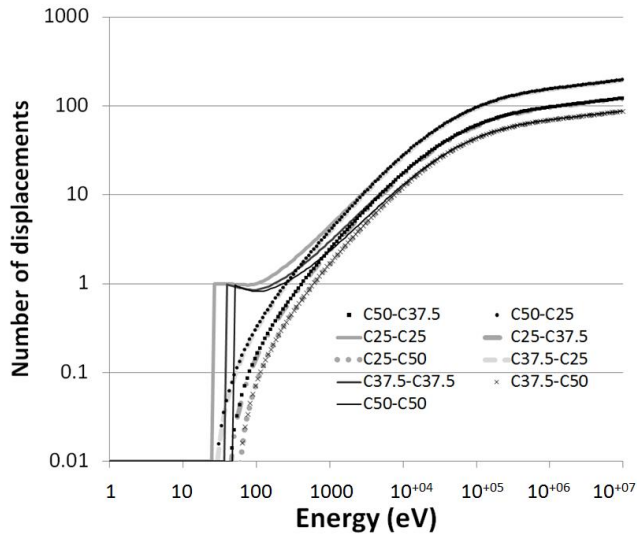


**Fig. 3.** Net displacement functions  $g_{ij}$  for Carbon material with three types of atoms having three different displacement energies (25 eV, 37.5 eV, and 50 eV). Interactions with recoils having different damage energies are shown.

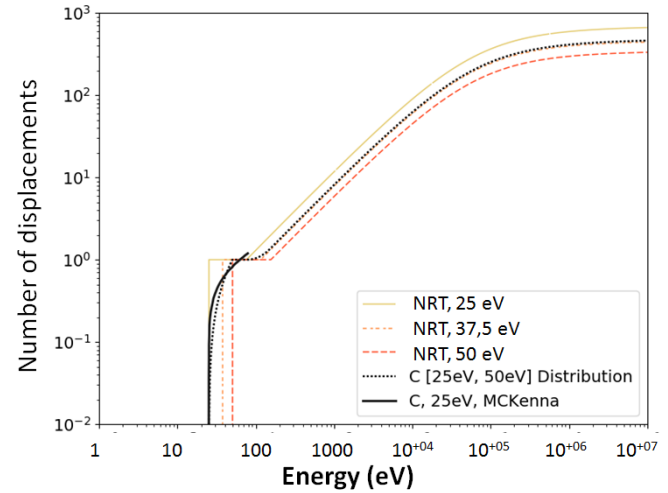


**Fig. 4.** NRT damage function ( $g_{ij}$ ) for carbon atoms having three different damage energies (25 eV, 37.5 eV, and 50 eV). Comparison is made with the damage function deduced from the integro-differential equation involving a uniform  $E^d$  distribution ranging from 25 eV up to 50 eV. MD data from McKenna [37] is also provided.

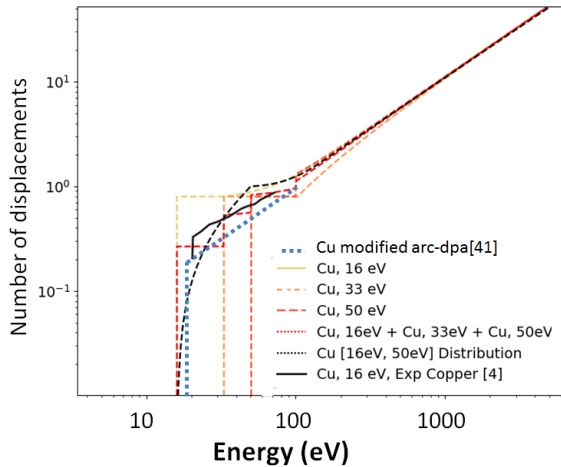


**Fig. 5.** NRT damage function ( $g_{ij}$ ) for copper atoms having three different damage energies (16 eV, 33 eV, and 50 eV). Comparison is made with the damage function deduced from the integro-differential equation involving a uniform  $E^d$  distribution ranging from 16 eV up to 50 eV. Comparison is made with the experimental data of ref. [4] and the modified arc-dpa expression from [41]. The case of a distribution having only three damage energies is also shown (three step function).

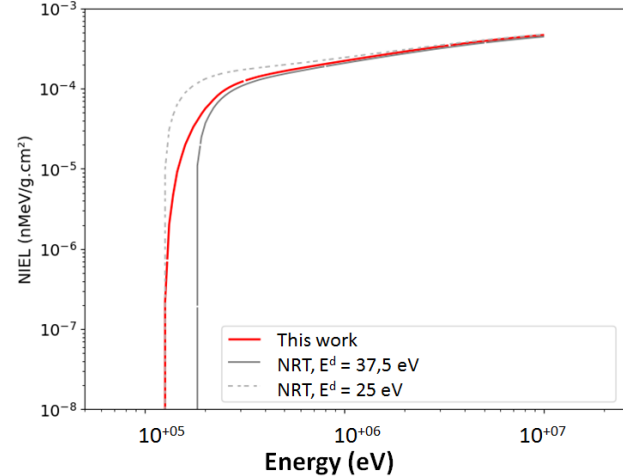


**Fig. 6.** NIEL of electrons in carbon material. Three cases are compared one calculation is based on NRT damage function using  $E^d = 25$  eV. A second analogous calculation uses  $E^d = 37.5$  eV. The red curve present the NIEL calculated using a damage function including an uniform damage energy distribution between 25 eV and 50 eV.

Mc Kenna [37] has calculated the net displacement damage function for graphite thanks to MD simulations. These authors proposed in the threshold region a net displacement function that depends on the square root of the PKA energy. This function is compared to our calculation in Fig. 4. The agreement with our calculation is quite good according to the rough assumptions made in our approach. It is interesting to note that the lack of step function in the threshold region can be well represented by a distribution probability of threshold displacement energy that ranges from 25 eV up to 50 eV the most currently admitted threshold displacement energy for carbon material. Similar calculations have been performed for copper target material (Fig. 5). The damage function of copper is compared on Fig. 5 with both experimental data provided in ref. [4] and the modified arc-dpa function proposed in ref. [41]. Here again the agreement between our approach and literature data is quite good.

In a second time the impact of the smooth increasing damage function on the NIEL of incident electrons has been analysed. The cases of heavier particles such as protons or heavy ions have been discarded because it is demonstrated that the threshold part of the displacement function does not impact significantly the NIEL on most of the energy range ( $> \sim 100$  eV) [40]. On a contrary the NIEL of electrons depends on the shape of the displacement damage function [40]. Indeed, The shape of the NIEL vs. Energy



curve of electrons is mainly driven by the recoil energy that can be transferred to PKAs and thus it is strongly dependent on the chosen threshold displacement damage energy. The impact of the displacement function of the NIEL of electrons in carbon material is shown in Fig. 4. The shape of the NIEL(E) curve is clearly affected by a change in the displacement function. The curve increases much more smoothly (Fig. 6).

## 6. Silicon target : Finding the most proper threshold energy distribution by comparison with experimental NIEL

### 6.1. Different damage distributions for correlation of the calculated NIEL with experimental damage factors.

The study has been extended to the case of silicon material for which experimental damage factors are available [42]. The calculated NIEL can be compared to these experimental data. This way, the best threshold energy distribution capable to reproduce the experimental damage factors measured on silicon devices can be identified. The resulting damage function will be discussed in a second time.

The NIEL is classically given by the following integral:

$$NIEL(E) = \eta \frac{2E_{min}^d}{0.8} \int_{E_{min}^d}^{Q_{max}} \frac{d\sigma}{dQ} \cdot n(Q) \cdot dQ \quad (13)$$

Where  $d\sigma/dQ$  is the differential interaction cross section. The McKinley & Feshbach correction of the Coulombian expression has been used for incident electrons [19].  $\eta$  is the atomic density of the irradiated material. This is a function of the net displacement damage function  $n(Q)$  introduced in previous sections.

Different basic damage distributions have been used for the NIEL calculation. Uniform, Normal, LogNormal and Weibull distributions with various set of parameters have been tested. First the case of different uniform probability distributions is shown Fig. 7 and Fig. 8. The damage energies spread respectively from 13 eV up to 74 eV, from 21 eV up to 99 eV and from 35 eV up to 120 eV. The impact of the distribution of displacement energy on the electron NIEL is shown in Fig. 8. We can observe on Fig. 8 the offset of the NIEL curves with the change in the damage energy distribution. The agreement with experimental damage factors is best when the threshold displacement energies are spread from 35 eV up to 120 eV, with an average damage energy of 77.5 eV. The experimental data presented in Fig. 8 are extracted from ref. [42]. Both dark current increase and short circuit current damage factors are presented. They have been measured on different silicon detectors with electrons in the energy range [500keV, 20 MeV]. Results obtained on two photodiodes and two image sensors are reported. The first diode is a P+N CANBERRA FD50-14-300RM Passivated Implanted Planar Silicon (PIPS) detector. The second photodiode is the Hamamatsu S1337-33BQ, Results obtained on two imagers are also shown. The first imager is a CMOS Image Sensor (CIS) Teledyne E2V EV76C560 Sapphire with 1.3 Mpixels ( $1024 \times 1280$ ). The second imager is the charge coupled device Teledyne E2V CCD47-20, an advanced inverted mode  $1024 \times 1024$  pixel full-frame. Both dark current and short circuit current measurements of all devices was performed at approximately room temperature.

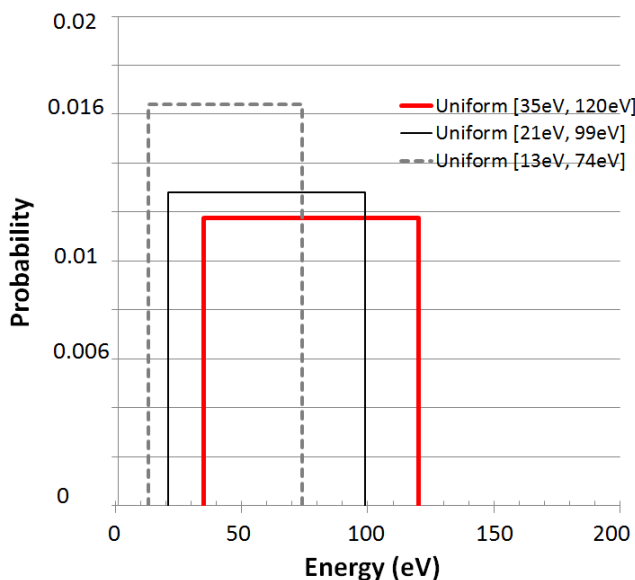


Fig. 7. Uniform threshold displacement damage energy tested for electron NIEL calculation in silicon.

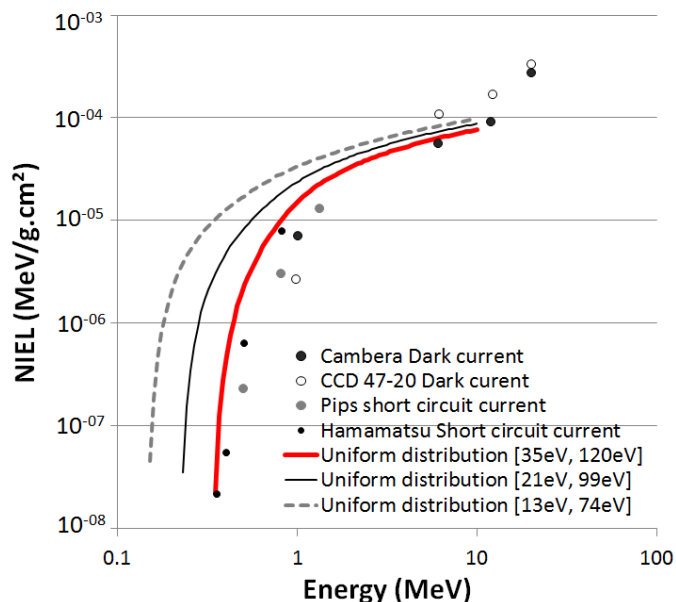


Fig. 8. NIEL of electrons in silicon for various uniform distributions.

Due to the mass difference between a recoil atom (~2000) and an incident electron, this latter needs an important energy to be able to displace this atom. In a silicon target, electrons need at least ~300 keV to displace a silicon recoil, if a threshold displacement energy of 21 eV is considered. Above some hundreds of keV and up to some MeV, it will be hard for electrons to displace atoms, and the capability for an incident electron to produce atomic displacements strongly depends on the threshold displacement energy. This makes the NIEL of electrons a relevant quantity to evaluate the threshold damage energy with a reasonable accuracy. Yet, the displacement threshold is known to depend on the crystallographic orientation. The variation from a direction to another can be quite large [36]. Including a distribution of displacement damage energy change significantly the displacement damage function near the threshold and consequently the NIEL of electrons in the range [~100 keV, ~MeV] (Fig. 8). By analogy, a change in the NIEL of heavier particle, such as protons, is expected to be seen only around some hundreds of eV (the minimum level of energy required to produce atomic displacements). For instance, in the space domain, where degradations are dominated by high energy protons having energies of several tens of MeV, this correction is negligible. This is not the case for electrons which are in the radiation belts in the energy range [keV, 10 MeV].

This analysis have been pushed further, by using Normal, LogNormal and Weibull distributions with different set of parameters (Fig. 9 & Fig.10). The Weibull distribution is defined as follow :

$$P(E^d) = \frac{s}{w} \left( \frac{E^d - th}{w} \right)^{s-1} e^{-\left( \frac{E^d - th}{w} \right)^s} \quad (14)$$

s is the shape parameter, w the scale parameter and th a threshold that define the energy domain of application of the probability distribution (>th).

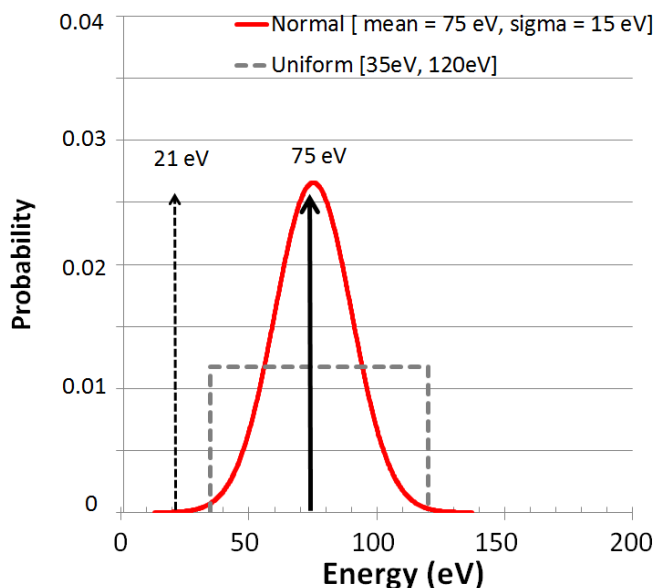


**Fig. 9.** Comparison of uniform and normal (mean = 75 eV, Std. Dev. = 15 eV) threshold displacement damage energy tested for electron NIEL calculation in silicon.

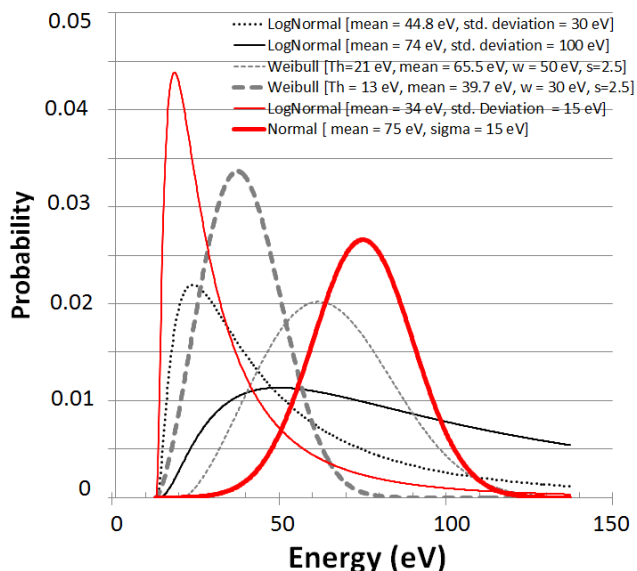


**Fig. 10.** Comparison of different damage energy distribution probability normal (mean = 75 eV, Std. Dev. = 15 eV), LogNormal (mean = 74 eV, 44.8 eV, 34 eV, Std. Dev. = 100 eV, 30 eV, 15 eV), Weibull distribution (th=13 eV, 21 eV, w = 30 eV, 50 eV and s = 2.5).

The impact of each of these distributions on the electron NIEL in silicon is shown in Figure 11 and Figure 12. The conclusion is similar to one given when considering the uniform distributions. The agreement with the experimental damage factor is better when the mean of the distribution is closer to 75 eV (Fig. 11 and Fig. 12). In a way it reaches the same conclusion as what is reported in [40] where an “effective” NIEL was estimated on the basis of MD simulation results. The calculated NIEL has been found to be closest to experimental damage factors for a Normal distribution having an average damage energy of 75 eV and a standard deviation of 15 eV. Comparisons with classical calculations performed with the NRT function presenting a single threshold damage energy of 21 eV and 75 eV are also presented in Fig.11. One can see that an average displacement damage energy larger than the commonly used value of 21 eV is best suited for the silicon NIEL calculation. [47] reports that the range found in both experimental and model-based studies for the threshold damage energy is between 10 eV and 30 eV, while [36] reports a minimum value of  $13\text{eV} \pm 3\text{eV}$ , an average value of  $37 \pm 7\text{eV}$  and an “effective” displacement energy of  $74 \text{eV} \pm 15\text{eV}$ . This latter value seems to be best appropriate, to reproduce the experimental damage factors reported in [42] (Fig. 11, Fig. 12).

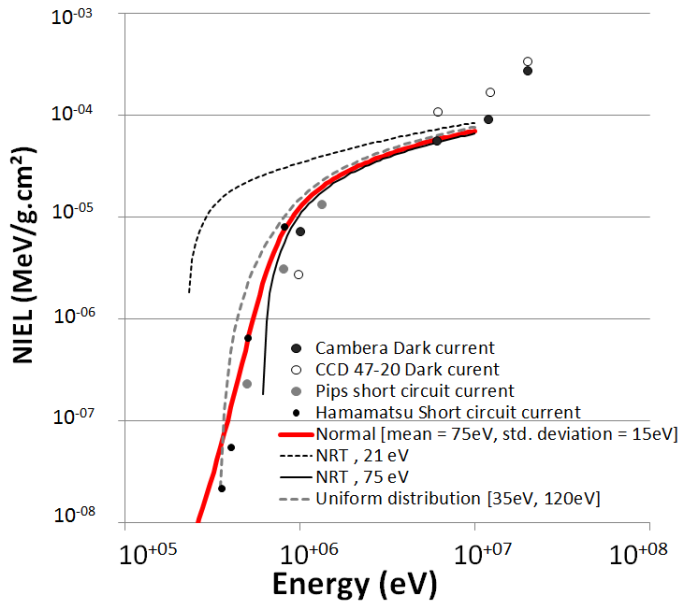


**Fig. 11.** NIEL of electrons in silicon for various damage energy distributions. Comparison is made between cases using some damage probability distribution (normal and uniform) and classical NRT approach based on 21 eV and 75 eV damage energy.

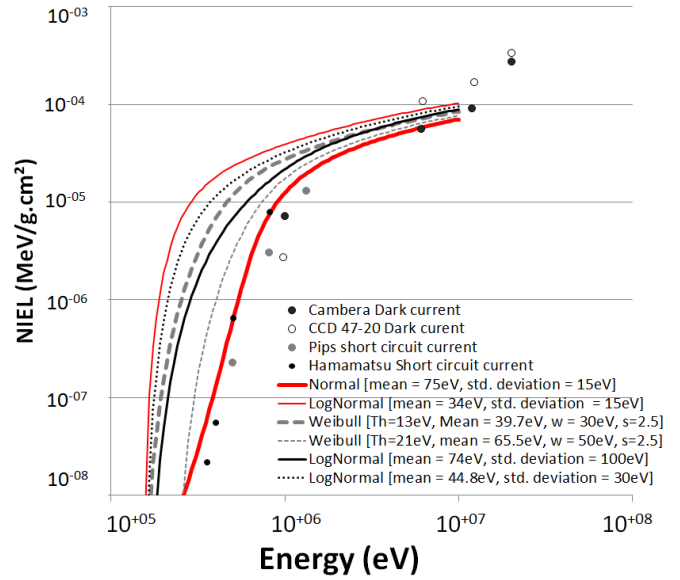


**Fig. 12.** Comparison of different damage energy distribution probability normal (mean = 75 eV, Std. Dev. = 15 eV), LogNormal (mean = 74 eV, 44.8 eV, 34 eV, Std. Dev. = 100 eV, 30 eV, 15 eV), Weibull distribution (th=13 eV, 21 eV, w = 30 eV, 50 eV and s = 2.5).

## 6.2. Damage functions calculated with the different threshold energy distributions

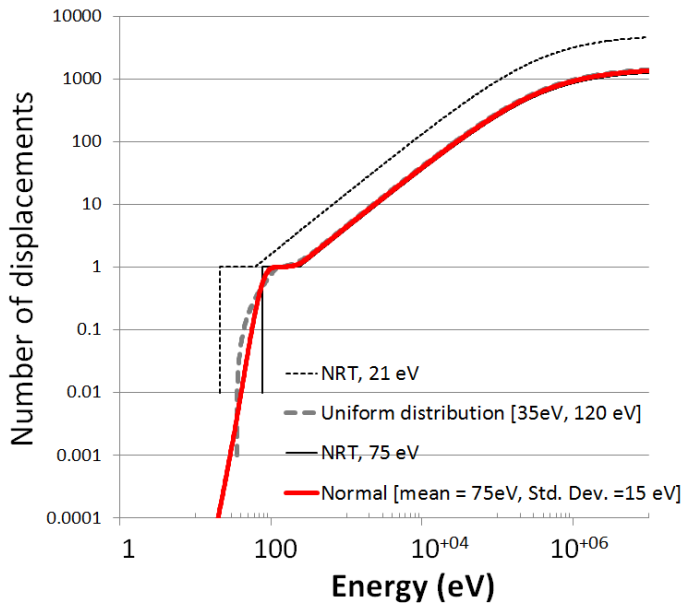


**Fig. 13.** Net displacement damage function ( $g_{ij}$ ) of silicon for a normal damage energy distribution (mean = 75 eV, Std. Dev. = 15 eV). Comparison is made with classical NRT damage function and a function based on the use of a uniform distribution in the range [35 eV, 120 eV].

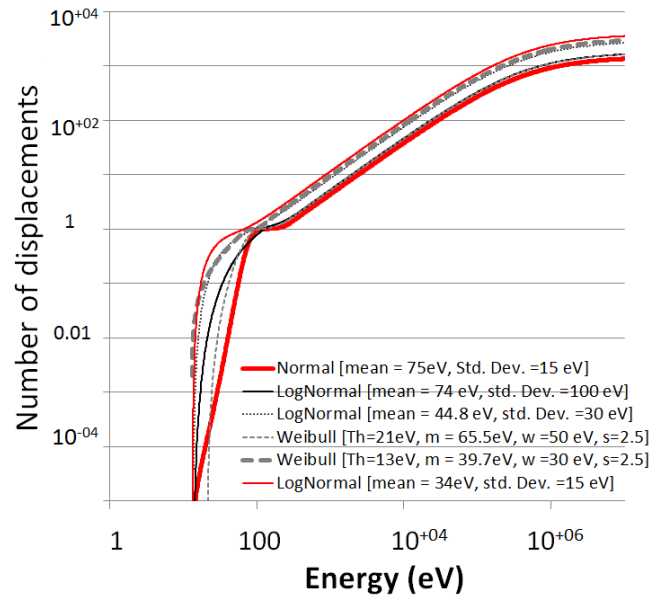


**Fig. 14** Net displacement damage function ( $g_{ij}$ ) for the various damage energy distributions. The damage function providing the best agreement between NIEL and experimental damage factors is provided by the Normal distribution having a mean of 75 eV and a standard deviation of 15 eV.

The damage functions deduced from the energy threshold distributions are reported in Fig. 13 and Fig. 14. The damage function best suited to reproduce the experimental damage factors is shown in thick red line on both figures. It corresponds to the modified NRT damage function calculated with a Normal distribution of mean 75 eV and standard deviation of 15 eV. The difference with the NRT function using a single  $E^d$  value of 21 eV is significant (Fig. 13). The average threshold energy of the distribution is the most impacting parameter. Both Uniform and Normal distributions leads to nearly the same damage function

when their average are comparable (Fig.13). Some more detailed comparisons are presented Comparisons in Fig. 14 for Normal, LogNormal and Weibull distributions. The Damage function becomes in the region of the threshold a smooth increasing function that can be represented by a power law. It is not so different from the results proposed in [41].

The method presented here, proposes to include in the classical NRT partitioning formalism, a distribution of threshold displacement energy to take into account the natural anisotropy existing in any crystallographic structure. Various threshold displacement energies are introduced to mimic the variation observed on this quantity as a function of the crystallographic orientation. It allows interpreting experimental damage factors of incident electrons that often deviate from the NIEL calculated classically with only a single displacement damage energy [40, 42]. But, this adjustment of the NRT formalism relies on some important assumptions. According to NRT, the damaging process is interpreted as a cascade of independent binary collision between PKAs and SKAs. The displacement is possible only if a given threshold energy is overpassed during the collision. The angular dependence of  $E^d$  is still relatively unexplored. An example is provided in ref. [39] for iron. An assumption on  $E^d$  angular dependence is thus needed. Different threshold damage energy distributions (uniform, normal, lognormal, Weibull) have been tested. The range of variation of  $E^d$  reported in ref. [36] for many materials, has been used to scale those distributions. But rigorously, extensive molecular dynamic simulations are required to define accurately the dependence of  $E^d$  on the crystallographic orientation. It can also be mentioned that the electronic energy loss is considered only to evaluate the fraction of the energy which is not imparted to atoms during the damage cascade. But it is known that this energy contributes to reduce the capability of a PKA to displace atoms thanks to heating processes [48-54]. This is especially important given the recent improvements within the stopping theory based on the use of first principle calculations [53, 54]. It would be interesting to include the impact of the ionization on the damage function. Furthermore, the NRT based approaches are only focused on the collisional phase of the displacement cascade and neglect some effects that arise during the thermalization phase [8]. At high knock-on atom energy, Frenkel pairs are produced closer to each other's, enhancing some recombination effects [8]. The arc-dpa model proposes a solution to include this effect within the NRT approach [8]. It would be interesting to combine the arc-dpa approach and the work presented here, to get a more accurate description of the NRT function on the whole energy range of PKAs.

## 7. Conclusion

The threshold damage energy is known to depend on the crystalline orientation. A single threshold damage energy is classically used in the NRT damage function. This energy can be chosen equal to the mean damage energy, averaged over all crystalline orientations. But, under this assumption, the NRT damage function is still a step function in the threshold region, while some MD simulations clearly show that the damage function increases smoothly in this region. This work proposes a method to introduce a distribution of damage energy in the calculation of both the damage function and the NIEL. It is a simple way to include the dependence of the threshold damage energy to the crystalline orientation. The calculation is based on the description of the damage cascade proposed by Parkin & Coulter [11]. Different damage energies are introduced in the integro-differential equation to account for the spread of these damage energies. Calculations have been performed for three different materials: carbon, copper and silicon. The calculated damage functions are found to be in satisfactory agreement with measured data for copper and molecular dynamic simulations for carbon. In both cases calculations made the assumption of uniformly distributed  $E^d$  values, in a range extending from a minimum and maximum values taken from compiled data of ref. [36]. For silicon the NIEL has been calculated assuming different density probability functions. Experimental damage factors measured on silicon devices are well reproduced assuming a normal distribution of mean 75 eV and a standard deviation of 15 eV. This approach could be upgraded by including in the formalism both the arc-dpa NRT function and the enhancement effect induced by the ionizing dose on the damage production process.

## References

- [1] F. Seitz, J.S. Koehler, Displacement of atoms during irradiation, in: F. Seitz, D. Turnbull (Eds.), *Solid State Physics*, 2, Academic Press, New York, 1956, p. 307.
- [2] P. Jung, Production of atomic defects in metals, in: H. Ullmaier (Ed.), *Crystal and Solid State Physics*, Vol. 25 of Landolt-börnstein, New Series III, Springer, Berlin, 1991, pp. 1-86. Ch. 1.
- [3] J. R. Srouf, Review of displacement damage effects in silicon devices, *IEEE Trans. Nucl. Sci.* 50 (3) (2003) 653–670.
- [4] Kai Nordlund, Steven J. Zinkle, Andrea E. Sand, Fredric Granberg, Robert S. Averback, Roger E. Stoller, Tomoaki Suzudo, Lorenzo Malerba, Florian Banhart, William J. Weber, c. Francois Willaime, Sergei L. Dudarev, David Simeone, Primary radiation damage: A review of current understanding and models *Journal of Nuclear Materials* 512 (2018) 450-479.
- [5] G.H. Kinchin, R.S. Pease, The displacement of atoms in solids by radiation *Rep. Prog. Phys.* 18 (1) (1955) 1.
- [6] M.T. Robinson, I.M. Torrens, Computer simulation of atomic-displacement cascades in solids in the binary-collision approximation, *Phys. Rev. B* 9 (12) (1974) 5008-5024.
- [7] M.J. Norgett, M.T. Robinson, I.M. Torrens, A proposed method of calculating displacement dose rates, *Nucl. Eng. Des.* 33 (1) (1975) 50-54
- [8] K. Nordlund, S.J. Zinkle, A.E. Sand, F. Granberg, R.S. Averback, R.E. Stoller, T. Suzudo, L. Malerba, F. Banhart, W.J. Weber, F. Willaime, S. Dudarev, D. Simeone, Improving atomic displacement and replacement calculations with physically realistic damage models, *Nat. Commun.* 9 (2018) 1084.
- [9] D.J. Bacon, F. Gao, Y.N. Osetsky, Computer simulation of displacement cascades and the defects they generate in metals, *Nucl. Instrum. Methods Phys. Res. B* 153 (1999) 87-98
- [10] A. Akkerman, J. Barak, M. B. Chadwick, J. Levinson, M. Murat, Y. Lifshitz, Updated NIEL calculations for estimating the damage induced by particles and gamma-rays in Si and GaAs, *Radiat. Phys. Chem.*, 62(4) (2001) 304.

- [11] D.M. Parkin and C.A. Coulter, Total and net displacement functions for polyatomic materials, *J. Nucl. Mater.*, 101 (1981) 261-276.
- [12] H. Huang and N.M. Ghoniem, Neutron displacement damage cross sections for SiC, *J. Nucl. Mater.* 199 (1993) 221-230.
- [13] W.J. Weber, R.E. Williford and K.E. Sickafus, Total displacement functions for SiC, *J. Nucl. Mater.* 244 (1997) 205-211.
- [14] H.L. Heinisch, L.R. Greenwood, W.J. Weber and R.E. Williford, Displacement damage cross sections for neutron-irradiated silicon carbide, *J. Nucl. Mater.* 307-311 (2002) 895-899.
- [15] S. R. Messenger, E. A. Burke, J. P. Summers, M. A. Xapsos, R. J. Walters, E. M. Jackson, B. D. Weaver, Non ionizing energy loss (NIEL) for heavy ions, *IEEE Trans. Nucl. Sci.*, 46 (6) (1999) 1595-1601.
- [16] M. Huhtinen, Simulation of non-ionizing energy loss and defect formation in silicon, *Nucl. Instr. & Meth. In Phys. Res. A*, 491(2002) 194-215.
- [17] S. R. Messenger, E. A. Burke, M. A. Xapsos, G. P. Summers, R. J. Walters, I. Jun, T. Jordan, NIEL for heavy ions : an analytical approach, *IEEE Trans. Nucl. Sci.*, 50(6) (2003) ) 1919-1923.
- [18] Insoo Jun, M. Xapsos, S. R. Messenger, E. A. Burke, R. Walters, Proton non ionising energy loss (NIEL) for device applications, *IEEE Trans. Nucl. Sci.*, 50 (6) (2003) 1924-1928.
- [19] C. Inguibert, R. Gigante, NEMO a code to compute NIEL of protons, neutrons, electrons and heavy ions, *IEEE Trans. Nucl. Sci.* 53 (4) (2006) 1967-1972.
- [20] I. Jun, Wousik Kim, and Robin Evans, Electron nonionizing energy loss for device applications, *IEEE Trans. Nucl. Sci.*, 56 (6) (2009) 3229-3235.
- [21] R.S. Averback, Atomic displacement processes in irradiated metals, *J. Nucl. Mater.* 216 (1994) 49.
- [22] M.J. Caturla, T. Diaz de la Rubia, G.H. Gilmer, Recrystallization of a planar amorphous-crystalline interface in silicon by low energy recoils: a molecular dynamics study, *J. Appl. Phys.* 77 (7) (1995) 3121.
- [23] T. Diaz de la Rubia, G.H. Gilmer, Structural transformations and defect production in ion implanted silicon: a molecular dynamics simulation study, *Phys. Rev. Lett.* 74 (13) (1995) 2507-2510
- [24] L.A. Marques, M.J. Caturla, H. Huang, T. Diaz de la Rubia, Molecular dynamics studies of the ion beam induced crystallization in silicon, *Mater. Res. Soc. Symp. Proc.* 396 (1994) 201.
- [25] L. A. Miller, D. K. Brice, A. K. Prinja, S. T. Picraux, Displacement threshold energies in Si calculated by molecular dynamics, *Physical Review B* 49 (24) (1994) 16953.
- [26] Maria E. Barone, and Dimitrios Maroudas, Defect-induced amorphization of crystalline silicon as a mechanism of disordered-region formation during ion implantation, *J. of Computer-Aided Materials Design*, 4 (1) (1997) 63-73.
- [27] D. Stiebel, A. Burenkov, P. Pichler, E Cristiano, A. Claverie, H. Ryssel, Modeling the Amorphization of Si due to the Implantation of As, Ge, and Si, *Ion Implantation Technology, 2000. Conference (2000)* 251-254.
- [28] L. A. Marques, L. Pelaz, J. Hernandez, J. Barbolla, Stability of defects in crystalline silicon and their role in amorphization, *Phys. Rev. B*, 64 (2001) 045214.
- [29] J. M. Hernandez-Mangas, J. Arias, L. Bailon, M. Jaraiz, J. Barbolla, Improved binary collision approximation ion implant simulators, *J. of Appl. Phys.*, 91 (2) (2002) 658.
- [30] L. Pelaz, L.A. Marques, J. Barbolla, Ion-beam-induced amorphization and recrystallization in silicon, *J. Appl. Phys.* 96 (11) (2004) 5947-5976.
- [31] K. Nordlund, J. Wallenius, L. Malerba, Molecular dynamics simulations of threshold energies in Fe, *Nucl. Instrum. Methods Phys. Res. B* 246 (2) (2006) 322-332.
- [32] L. A. Marques, L. Pelaz, P. Lopez, I. Santos, M. Aboy, Recrystallization of atomically balanced amorphous pockets in Si : a source of point defects, *Physical Review B*, 76 (2007) 153201.
- [33] T. Jarrin, A. Jay, M. Raine, N. Mousseau, A. Hémerlyck, N. Richard, Simulation of Single Particle Displacement Damage in Si<sub>1-x</sub>Ge<sub>x</sub> Alloys—Interaction of Primary Particles With the Material and Generation of the Damage Structure, *IEEE Trans. on Nucl. Sci.* 67 (7) (2020) 1273-1283.
- [34] E. Holmström, A. Kuronen, K. Nordlund, Threshold defect production in silicon determined by density functional theory molecular dynamics simulations, *Phys. Rev. B* 78 (4) (2008), 045202.
- [35] K. Nordlund, in: *Proceedings of Summary Report of the Second Re- search Coordination Meeting*, 29 June–2 July 2015, IAEA Headquarters, Vienna, Austria, 2015, p. 19. INDC(NDS) 0691, December, <https://www-nds.iaea.org/publications/indc/indc-nds-0691.pdf>.
- [36] A.Yu.Konobeyev, U.Fischer, Yu.A.Korovin, S.P.Simakova, Evaluation of effective threshold displacement energies and other data required for the calculation of advanced atomic displacement cross-sections, *Nuclear Energy and Technology*, 3 (3) (2017) 169-175.
- [37] A.J. McKenna, T. Trevethan, C.D. Latham, P.J. Young, M.I. Heggie, Threshold displacement energy and damage function in graphite from molecular dynamics, *Carbon* 99 (2016) 71-78.
- [38] Benjamin J. Cowen, Mohamed S. El-Genk, Probability-based threshold displacement energies for oxygen and silicon atoms in  $\alpha$ -quartz silica, *Computational Materials Science* 117 (2016) 164–171.
- [39] P. Olsson, C. S. Becquart & C. Domain, Ab initio threshold displacement energies in iron, *Mat. Res. Lett.*, 4 (4) (2016) 219–225.
- [40] C. Inguibert, P. Arnolda, T. Nuns, G. Rolland, Effective NIEL in Silicon: Calculation using molecular dynamic results, *IEEE Trans. Nucl. Sci* 57 (4) (2010) 1915-1923.
- [41] Qigui Yang and Pär Olsson, Full energy range primary radiation damage model, *Phys. Rev. Mat.* (5) (2021) 073602.
- [42] T. Nuns, C. Inguibert, S. Soonckindt, B. Dryer, T. Buggiey, C. Poivey, Experimental Study of the NIEL Scaling for Silicon Devices, *Proceedings of the 18<sup>th</sup> International Conference on Radiation and its Effects on Components and Systems (RADECS 2018)*, Gothenburg, Sweden, September 16-21, 2018. DOI: 10.1109/RADECS45761.2018.9328677.
- [43] J.F. Ziegler, J.P. Biersack and U. Littmark, *The Stopping and Range of Ions in Solids*, Pergamon Press, New York (1985).
- [44] SRIM - The Stopping and Range of Ions in Matter [Online]. Available : <http://www.srim.org> Accessed July 20, 2021.
- [45] Q. Ran, Y. Zhou, Y. Zou, J. Wang, Z. Duan, Z. Sun, B. Fu, S. Gao, Molecular dynamics simulation of displacement cascades in cubic silicon carbide, *Nuc. Mat. And Energy* 27 (2021) 100957.
- [46] S.J. Zinkle, C. Kinoshita, Defect production in ceramics, *J. Nucl. Mater* 251 (1997) 200-217.
- [47] Patrick J. Griffin, Uncertainty in Silicon Displacement Damage Metrics due to the Displacement Threshold Treatment, *Proceedings of the 16<sup>th</sup> International Conference on Radiation and its Effects on Components and Systems (RADECS 2016)*, Bremen Germany, DOI: 10.1109/RADECS.2016.8093101.
- [48] A. Caro and M. Victoria, Ion-electron interaction in molecular-dynamics cascades, *Phys. Rev. A* 40 (5) (1989) 2287-2291.
- [49] Dmitriy S. Ivanov and Leonid V. Zhigilei, Combined atomistic-continuum modeling of short-pulse laser melting and disintegration of metal films, *Phys. Rev. B* 68 (2003) 064114.
- [50] D M Duffy, and A M Rutherford, Including the effects of electronic stopping and electron–ion interactions in radiation damage simulations, *J. of Phys.: Cond. Matt.*, 19 (1) (2006) 016207.
- [51] E Zarkadoula, S L Daraszewicz, D M Duffy, M A Seaton, I T Todorov, K Nordlund, M T Dovel and K Trachenko, Electronic effects in high-energy radiation damage in iron, *J. of Phys.: Cond. Matt.*, 26 (8) (2014) 085401.
- [52] E. Zarkadoula, G. Samolyuk, H. Xue, H. Bei, W. J. Weber, Effects of two-temperature model on cascade evolution in Ni and NiFe, *Scripta Materialia*, 124 (2016) 6-10.
- [53] E. Zarkadoula, G. Samolyuk, Y. Zhang, W. J. Weber, Electronic stopping in molecular dynamics simulations of cascades in 3C–SiC, *J. Nucl. Mater.*, 540 (2020) 152371.
- [54] Andrea E. Sand , Rafi Ullah, and Alfredo A. Correa, Heavy ion ranges from first-principles electron dynamics, *npj computational material*, 43 (2019)